

# Theory of cell sorting

Milton Nogueira  
Jan Jansen

Correspondence:  
m.nogueira.da.silva.junior@gmail.  
leidenuniv.nl, Master student,  
Leiden University,  
Full list of author information is  
available at the end of the article  
\*Equal contributor

## Abstract

In this project we will explore the kinetics of cell sorting and study if and how modifications and extensions of the standard cellular Potts model will change it.

**Keywords:** Cellular Potts Model; Adhesion energy; Cytoskeletally-driven membrane fluctuations

## Introduction

The cellular Potts model is a generalization of the Ising model in statistical mechanics used to study ferromagnetism [3]. The cellular Potts model was introduced by Glazier and Graner [1] with which they could simulate the sorting of biological cells and show a variety of emergent behavior of interacting cells. Grounded on the differential adhesion hypothesis, they proposed an energy functional for the system that is minimized as cells properly sort themselves. Subsequently, the model has been extended accordingly to address several biological questions[4]. This report is organized as follows. First, we introduce a modified Hamiltonian. Secondly, we bring up some results of our simulations in line with the scope of the project. Lastly, we conclude the report by touching upon some questions risen during the course of the simulations and by providing a concise discussion hereof.

## A relaxation of the Cellular Potts Model

There is, in fact, enough empirical evidence in the literature to support the claim that cells of different categories have indeed an average size. This property has been successfully explored in the context of the Cellular Potts Model [1, 4] to simulate the motility of interacting cells and to predict the emergent behavior at the tissue level. In fact, the model rests heavily upon the hypothesis that cells strive to achieve a target area [2]. In this project, we have proposed a relaxation of this hypothesis.

### The Hamiltonian

Under the Differential adhesion Hypothesis, we introduce the following Hamiltonian

$$H = \sum_{\vec{x}} \sum_{\vec{x}' \in \mathcal{M}(\vec{x})} J_{\tau(\sigma(\vec{x})), \tau(\sigma(\vec{x}'))} (1 - \delta_{\sigma(\vec{x}), \sigma(\vec{x}')} ) + \lambda \sum_{\text{spins } \sigma} \min_{\delta \in [-B; B]} (a_{\sigma} - A_{\tau(\sigma)} + \delta)^2, \quad (1)$$

where  $J_{\tau(\sigma(\vec{x})), \tau(\sigma(\vec{x}'))}$  stands for the adhesion energy of the interacting cells;  $\vec{x}$  represent a lattice site which resembles the position of biological cells;  $\sigma(\vec{x})$  gives the indices of identical cells;  $\mathcal{M}(\vec{x})$  is the extension of the local interactions among

cells<sup>[1]</sup>;  $\tau(\sigma(\vec{x}))$  represents the cell type of  $\sigma(\vec{x})$ ;  $A_{\tau(\sigma)}$  is the target area of a particular cell type and  $\lambda$  is the strength of this area constraint. The relaxation  $B > 0$  is a new parameter, which can be interpreted as the range of the energy penalty due to cell's deviation from a designated target area<sup>[2]</sup>.

A convenient way of writing (1) is

$$H_\beta = \sum_{\vec{x}} \sum_{\vec{x}' \in \mathcal{M}(\vec{x})} J_{\tau(\sigma(\vec{x})), \tau(\sigma(\vec{x}'))} (1 - \delta_{\sigma(\vec{x}), \sigma(\vec{x}')} ) + \tilde{\lambda} \sum_{\text{spins } \sigma} \min_{\tilde{\delta} \in [-\beta; \beta]} (\tilde{a}_\sigma - 1 + \tilde{\delta})^2, \quad (2)$$

where  $\tilde{\lambda} = \lambda A_{\tau(\sigma)}^2$ ,  $\tilde{a}_\sigma = a_\sigma / A_{\tau(\sigma)}$ ,  $\tilde{\delta} = \delta / A_{\tau(\sigma)}$ , and

$$\beta = B / A_{\tau(\sigma)}. \quad (3)$$

Moreover we also define

$$H_\beta^{\text{adhesion}} = \sum_{\vec{x}} \sum_{\vec{x}' \in \mathcal{M}(\vec{x})} J_{\tau(\sigma(\vec{x})), \tau(\sigma(\vec{x}'))} (1 - \delta_{\sigma(\vec{x}), \sigma(\vec{x}')} ), \quad (4)$$

and

$$H_\beta^{\text{volume}} = \tilde{\lambda} \sum_{\text{spins } \sigma} \min_{\tilde{\delta} \in [-\beta; \beta]} (\tilde{a}_\sigma - 1 + \tilde{\delta})^2. \quad (5)$$

Drawing on definitions (4) and (5), for each  $\beta$ , one has that

$$H_\beta = H_\beta^{\text{adhesion}} + H_\beta^{\text{volume}}. \quad (6)$$

If we take  $0 \leq B \leq A_{\tau(\sigma)}$  then

$$0 \leq \beta \leq 1, \quad (7)$$

and the family of Hamiltonians

$$\mathcal{H} = \{H_\beta : 0 \leq \beta \leq 1\} \quad (8)$$

must satisfy

$$\lim_{\beta \rightarrow 0^+} H_\beta = H_{\text{Glazier-Graner}}, \quad (9)$$

where

$$H_{\text{Glazier-Graner}} = \sum_{\vec{x}} \sum_{\vec{x}' \in \mathcal{M}(\vec{x})} J_{\tau(\sigma(\vec{x})), \tau(\sigma(\vec{x}'))} (1 - \delta_{\sigma(\vec{x}), \sigma(\vec{x}')} ) + \lambda \sum_{\text{spins } \sigma} (a_\sigma - A_{\tau(\sigma)})^2, \quad (10)$$

---

<sup>[1]</sup>Here we use a Moore neighborhood.

<sup>[2]</sup>"B" stands for the "Targetband" in the code.

and

$$\lim_{\beta \rightarrow 1^+} H_\beta = \sum_{\vec{x}} \sum_{\vec{x}' \in \mathcal{M}(\vec{x})} J_{\tau(\sigma(\vec{x})), \tau(\sigma(\vec{x}'))} (1 - \delta_{\sigma(\vec{x}), \sigma(\vec{x}'))} + \lambda \sum_{spins, \sigma} (a_\sigma)^2. \quad (11)$$

Therefore, if we draw upon (9) then, for  $\beta$  sufficiently small, we expect to reproduce the same results found in [1]. On the other hand, (11) means that for  $\beta \approx 1$ , one has that the adhesion strength will be the driving force of the system and our simulations should be consistent with this claim.

### 0.1 Procedure

The simulated cells are of two types, red cells, which we will refer to as  $r$ , and the yellow cells which we will refer to as  $y$ . Besides that, we refer to the medium, wherein these cells exist, as  $m$ . Hence,  $\tau(\vec{x})$  can assume three values  $r$ ,  $y$ , and  $m$ .

To mimic cytoskeletally-driven membrane fluctuations, for each  $0 \leq \beta \leq 1$ , we repeatedly attempt to replace the index  $\sigma$  of a randomly chosen lattice  $\vec{x}$  by the one of a random lattice site  $\vec{x}' \in \mathcal{M}(\vec{x})$ . At each Monte Carlo step in the simulation, we convert the index with probability

$$P(\Delta H_\beta) = \begin{cases} \exp(-\Delta H_\beta/T), & \Delta H_\beta > 0; \\ 1, & \Delta H_\beta \leq 0; \end{cases}$$

for  $T > 0$ , and with probability

$$P(\Delta H_\beta) = \begin{cases} 0, & \Delta H_\beta > 0; \\ 0.5, & \Delta H_\beta = 0; \\ 1, & \Delta H_\beta < 0; \end{cases}$$

for  $T = 0$ .

## Results

**Simulations:**  $\beta \approx 0$

As we have justified in the previous section, for  $\beta = 0$  and, in fact, for  $\beta$  sufficiently small, we hope to recover the same results found by [1]. Indeed, for  $\beta = 0$  and  $\beta = 0.014$ , we see in the Figure 1 that there is a slightly difference between the simulations, but yet the pattern behavior is very similar. Likewise, for  $\beta = 0.014$ , see Figure 2, we could reproduce very similar patterns as in the Glazier-Graner Model. These simulations have shown that our approach is consistent.

**Simulation:**  $0.286 \leq \beta \leq 1$

Insofar as  $\beta$  tends to 1, we observe that *adhesion* becomes the driving force of the system. If this is the case then, under the Differential Adhesion Hypothesis, one has that the cells will prefer to shrink seeing that, in doing so, the Hamiltonian decreases. In fact, for  $\beta \geq 0.286$ , see Figure 3, we see that the two clusters of yellow cells have become smaller compared to the first simulation for  $\beta = 0.014$ . This is much clearer for  $\beta = 0.786$ , for which one of the initially formed cluster of yellow cells dissolves into the medium after few MCS. For  $\beta = 0.857$ , one has that all the

cells die out. An intuitive argument for this rests upon the Hamiltonian. In fact, as we have seen in the section 2, for  $\beta \approx 1$ , one has that

$$H_\beta \approx \sum_{\vec{x}} \sum_{\vec{x}' \in \mathcal{M}(\vec{x})} J_{\tau(\sigma(\vec{x})), \tau(\sigma(\vec{x}'))} (1 - \delta_{\sigma(\vec{x}), \sigma(\vec{x}')} ) + \lambda \sum_{spins, \sigma} (a_\sigma)^2. \quad (12)$$

Hence, it is more energetically favorable for the system if the term

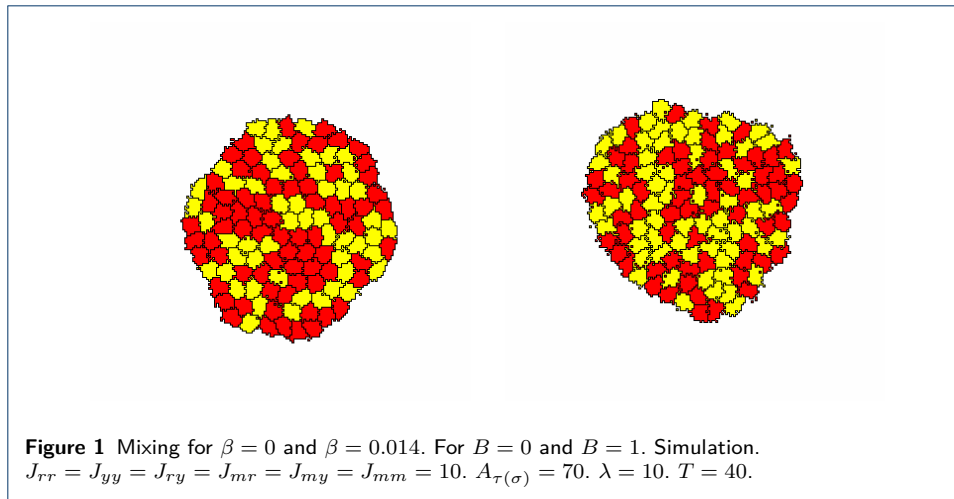
$$\lambda \sum_{spins, \sigma} (a_\sigma)^2 \quad (13)$$

decreases. As for the red cells, due to their low adhesion, they mix better with the medium which causes them to dissolve into it faster. Under the DAH, they will shrink until they disappear because a decrease in the cellular boundary elements will certainly cause the Hamiltonian to diminish.

In line with the scope of this project, we have also simulated for "Mixing", see Figure 4, with different values of the dimensionless parameter  $\beta$ . As the cells adhere equally well to each other, under the DAH, they prefer to cling onto each other seeing that it prevents them from increasing the boundary elements which, in turn, would cause the Hamiltonian to increase. Moreover, insofar as  $\beta$  approaches 1, the system goes toward configurations in which the cluster of cells becomes smaller. In fact, if we draw on (13) then we can easily see that this is more energetically favorable for the system. For  $\beta = 0.743$ , the cells start dissolving into the medium after few MCS.

#### Simulation: $T = 0$

For  $\beta = 0$ , we have already seen that we recover the Glazier-Graner model. In fact, if  $T = 0$  then the system gets stuck at a local minimum and, at  $T = 0$ , it is unlikely for the system to escape from such a configuration. This happens because all the systems states, within a small neighborhood of this minimum, have a higher energy. Regarding the simulations, it implies that the system will remain frozen. On the other hand, for the modified Hamiltonian  $H_\beta$ , with  $\beta > 0$ , not all the cells are penalized with respect to the area constraint. This implies that the system kinetics will change considerably. To illustrate that, we have simulated with cells adhering equally well to each other (see Figure 5). For  $\beta = 0$ , at  $T = 0$ , once the minimum has been found, the system prefers to remain frozen and a boundary cell neither moves inward through the cluster of cells nor outward through the medium. This is because it could generate an increase in cellular boundary elements which, in turn, would cause  $H_{GLazier-Graner}$  to become higher. However, for  $0 < \beta \leq 1$ , we see in the simulations that the dynamics of the system changes significantly on the boundary. Due to the relaxation of the area constraint, we see that the cells on the boundary may take up the space in the medium seeing that it can now cause  $H_\beta^{volume}$  to decrease. However, this is also compensated with a decrease in volume size seeing that it also guarantees that  $H_\beta^{adhesion}$  decreases what results in a lower  $H_\beta$ . The cells inside the cluster, away from the boundary, prefer to shrink and barely take up each other's space as it is still energetically more favorable for the system.



Therefore, the kinetics of the systems can be reduced to an active boundary whose elements keep dissolving into the medium. As the parameter  $\beta$  approaches 1, one has that  $H_{\beta}^{adhesion}$  becomes the main driving force and the cells dissolve faster into the medium until all the cells disappear.

## Discussion

In this project, we have provided a modification of the Glazier-Graner Hamiltonian. The results are consistent with the simulations performed in [1] for low values of the parameter  $\beta$ . For higher values of  $\beta$ , the system goes through a lot of different phenotypes before it finally undergoes total apoptosis. At  $T = 0$ , different from the simulations performed with the original Hamiltonian, i.e., for  $\beta = 0$ , we could free the system from getting stuck at a local minimum. Indeed, at  $T = 0$ , we have simulated an active cellular boundary leading the system to total apoptosis. As for the limitations, we can say that the modification does not lead us to properly get cell sorting because its dynamics is at the expense of structure. However, we can exhibit lots of "phenotypes" by varying the parameter  $\beta$  when cell is undergoing apoptosis, which might shed light on some interesting biological questions. As for the future, we can explore the family (8) and examine if interesting phenotypes, which might match experimental observations, can arise from it.

## Program Code

We used software Tissue Simulation Toolkit, version /TST0.1.4.2.tar.gz, downloaded from: <http://sourceforge.net/projects/tst/> We made some small changes in this code all marked with "Milton & Jan". For the modified code see the annex.

Program listings or program commands in the text are normally set in typewriter font, e.g., CMTT10 or Courier.

*Main modification in ca.cpp*

---

```
/* Milton & Jan main modification. */
gemeten=0;
```

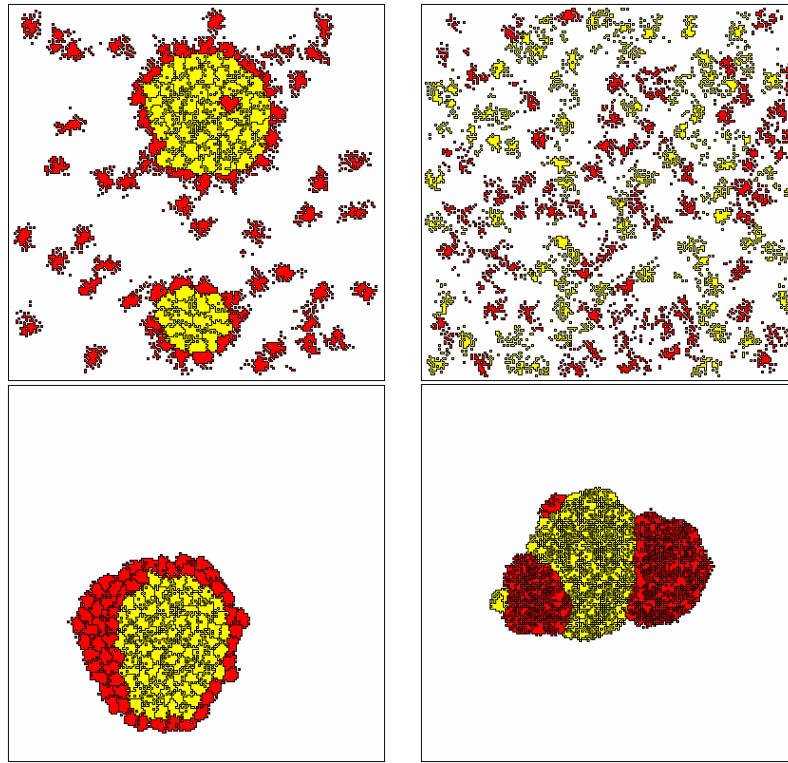


**Figure 2** Dispersal.  $\beta = 0.014$ .  $B = 1$ . Simulation.

$J_{rr} = 14$ ;  $J_{yy} = 4$ ;  $J_{ry} = 9$ ;  $J_{mr} = 2$ ;  $J_{my} = 16$ ;  $J_{mm} = 0$ .  $A_{\tau(\sigma)} = 70$ .  $\lambda = 10$ .  $T = 40$ . Cell mixing with the medium.  $\beta = 0.014$ .  $B = 1$ . Simulation.

$J_{rr} = 10$ ;  $J_{yy} = 20$ ;  $J_{ry} = 10$ ;  $J_{mr} = 1$ ;  $J_{my} = 1$ ;  $J_{mm} = 0$ .  $A_{\tau(\sigma)} = 70$ .  $\lambda = 10$ .  $T = 40$ .

Engulfment.  $\beta = 0.014$ .  $B = 1$ . Simulation.

$J_{rr} = 8$ ;  $J_{yy} = 5$ ;  $J_{ry} = 9$ ;  $J_{mr} = 10$ ;  $J_{my} = 15$ ;  $J_{mm} = 0$ .  $A_{\tau(\sigma)} = 70$ .  $\lambda = 10$ .  $T = 40$ . Cell mixing with the medium.  $\beta = 0.014$ .  $B = 1$ . Simulation.

$J_{rr} = 10$ ;  $J_{yy} = 20$ ;  $J_{ry} = 10$ ;  $J_{mr} = 1$ ;  $J_{my} = 1$ ;  $J_{mm} = 0$ .  $A_{\tau(\sigma)} = 70$ .  $\lambda = 10$ .  $T = 40$ . Cell sorting (Tumor invasion).  $\beta = 0.014$ .  $B = 1$ . Simulation.

$J_{rr} = 1$ ;  $J_{yy} = 1$ ;  $J_{ry} = 10$ ;  $J_{mr} = 10$ ;  $J_{my} = 10$ ;  $J_{mm} = 0$ .  $A_{\tau(\sigma)} = 70$ .  $\lambda = 10$ .  $T = 40$ .

```

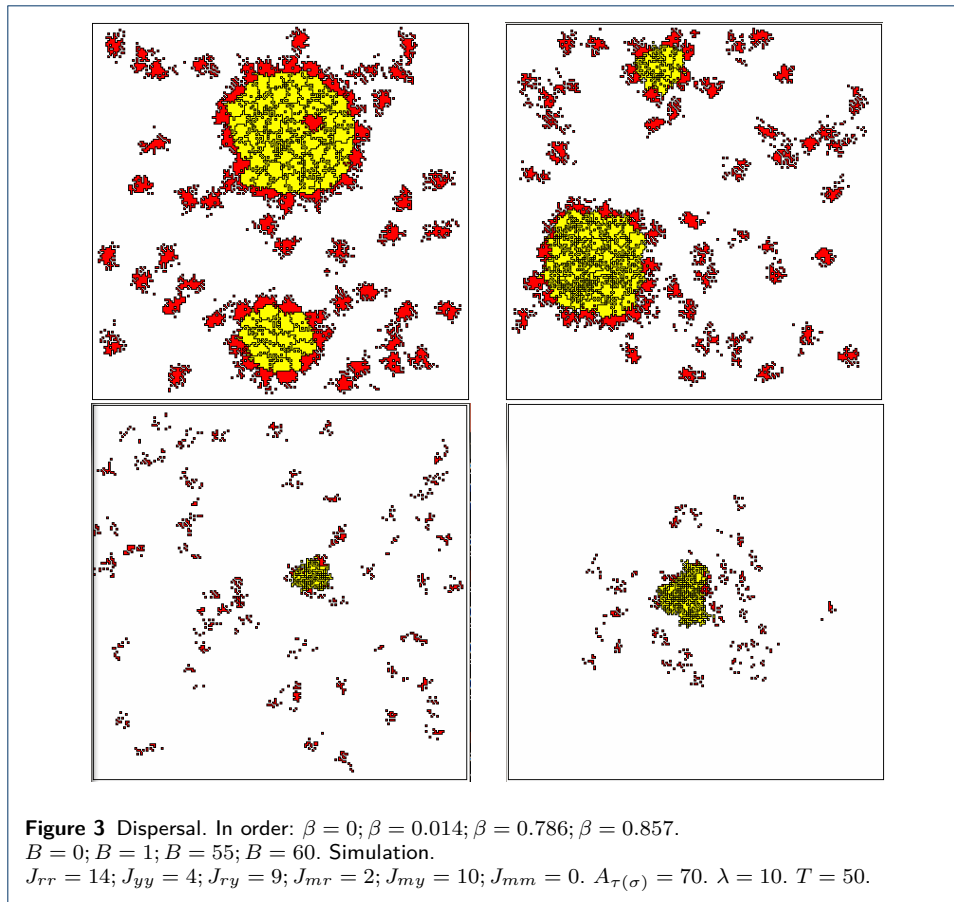
if ( sxyp == MEDIUM ) {
    gemeten=1;
    if ( ( (*cell)[sxy].Area() - (*cell)[sxy].TargetArea())^2 >
        Targetband^2 ){

        DH += (int)(par.lambda * (1. - 2. * (double) ( (*cell)[sxy].Area() -
            (*cell)[sxy].TargetArea()+Targetband) ));
    };//if ( ( (*cell)[sxy].Area()
} //if ( sxyp == MEDIUM ) {

if ( sxy == MEDIUM && gemeten==0){ gemeten=2;
    if ( (((*cell)[sxyp].Area() - (*cell)[sxyp].TargetArea())^2 > Targetband^2 ) {
        DH += (int)((par.lambda * (1. + 2. *
            (double) ( (*cell)[sxyp].Area() -
            (*cell)[sxyp].TargetArea()-Targetband) )));
    } // if ( ( (*cell)[sxyp].Area() -
} // if ( sxy == MEDIUM && gemeten==0 &&

else if (gemeten==0){

```



```

if ( ( ( (*cell)[sxyp].Area() - (*cell)[sxyp].TargetArea())^2 >
      Targetband^2 )) {
  DH += (int)((par.lambda * (2. + 2. * (double)
    ( (*cell)[sxyp].Area() - (*cell)[sxyp].TargetArea()-Targetband
      ) )));
} //if ( ( ( (*cell)[sxyp].Area() -
if ((((*cell)[sxy].Area() - (*cell)[sxy].TargetArea())^2 > Targetband^2 )) {
  DH += (int)((par.lambda * (2. + 2. * (double)
    ( - (*cell)[sxy].Area() + (*cell)[sxy].TargetArea()-Targetband ))
      ));
} // if if ((((*cell)[sxy].Area() -
} // else if (gemeten==0 )

/* End of main modification by Milton & Jan */

```

#### References

1. James A. Glazier and François Graner: Simulations of the differential adhesion driven rearrangement of Biological cells. *Physical Review E*, vol. 47, 3 (1993).
2. Anja Voss-Böhme: Multi-scale modelling in morphogenesis: a critical analysis of the Cellular Potts Model. *Plos(one)*, vol. 7, issue 9 (2012).
3. E. Ising: Beitrag zur Theorie des Ferromagnetismus. *Z. Physik*, vol. 31, 253-258 (1925).
4. Roeland M. H. Merks, Stuart A. Newman, James A. Glazier: Cell-Oriented Modeling of In Vitro Capillary Development. *Cellular Automata*, Vol. 3305, 425-434 (2004).
5. Roeland M.H. Merks, Michael Guravage, Dirk Inze, and Gerrit T.S. Beemster *VirtualLeaf: An Open-Source Framework for Cell-Based Modeling of Plant Tissue Growth and Development*, *Plant Physiology A*, 155:656-666, 2011.

